HUMAN GENE THERAPY 18:367–378 (April 2007)

DOI: 10.1089/hum.2006.139

Engineering Adeno-Associated Virus for One-Step Purification via Immobilized Metal Affinity Chromatography

JAMES T. KOERBER,[1] JAE-HYUNG JANG,[1] JULIE H. YU,[1] RAVI S. KANE,[2] and DAVID V. SCHAFFER[1]

ABSTRACT

Adeno-associated virus (AAV) is a promising vehicle for gene therapy, which will rely on the generation of high-titer, high-purity recombinant vectors. However, numerous purification protocols can involve challenging optimization or scalability issues, and most AAV serotypes do not bind heparin or sialic acid, used for AAV2/3 or AAV4/5 purification, requiring the development of new chromatography strategies. Immobilized metal affinity chromatography (IMAC) allows for robust protein purification via affinity tags such as the hexahistidine (His_6) sequence. Through the combination of a diverse AAV2 library and rational peptide insertions, we have located an optimal His_6 tag insertion site within the viral capsid. This mutant and a related AAV8 variant can be purified from clarified cell lysate in a single gravity column step at infectious particle yields exceeding 90%. Furthermore, injection of IMAC-purified vector into the brain demonstrates that it mediates high-efficiency gene delivery *in vivo*, equivalent to that of wild-type capsid, with minimal immune cell activation. This affinity chromatography method may offer advantages in ease of purification, final vector purity, and process scalability. Moreover, a combined rational design and high-throughput library selection approach can aid in the design of enhanced viral gene delivery vectors.

OVERVIEW SUMMARY

Adeno-associated virus (AAV) is promising a vehicle for gene therapy. However, numerous purification protocols can involve challenging optimization or scalability issues. Immobilized metal affinity chromatography (IMAC) allows for robust protein purification via affinity tags such as the hexahistidine (His_6) sequence. Through the combination of a diverse AAV2 library and rational peptide insertions, we have generated a novel AAV2 and the first reported AAV8 mutants that contain a His_6 tag, which facilitates one-step purification via an immobilized metal affinity gravity column at yields exceeding 90%. These variants retain near wild-type gene delivery efficiency and titers on numerous cell lines *in vitro*. Furthermore, injection of IMAC-purified vector into the brain demonstrates that it mediates high-efficiency gene delivery *in vivo*, equivalent to that of wild-type capsid, with minimal immune cell activation. This affinity chromatography method may offer advantages in ease of purification, final vector purity, and process scalability.

INTRODUCTION

ADENO-ASSOCIATED VIRUS (AAV) is a nonpathogenic human parvovirus that requires a helper virus to replicate (Fields *et al*., 2001). The single-stranded 4.6-kb DNA genome of AAV contains two open reading frames (ORFs): *rep*, which encodes a set of four proteins (Rep78, Rep68, Rep52, and Rep40) essential for replication of the viral genome, and *cap*, which encodes the structural proteins (VP1–VP3) (Srivastava *et al*., 1983; Samulski *et al*., 1989). VP1–VP3 self-assemble into the viral icosahedral capsid, 25 nm in diameter, into which the genome is inserted (Fields *et al*., 2001). The capsid then escorts the viral genome through numerous gene delivery barriers, from the point of entry into tissue to the final viral destination in a target cell nucleus. This high delivery efficiency has been harnessed for gene delivery to and long-term gene expression in a broad array of dividing and nondividing cell types *in vivo* (Flotte *et al*., 1993; Kaplitt *et al*., 1994; Kaspar *et al*., 2003). Natural evolution has generated >100 AAV serotypes, which exhibit a diverse array of gene delivery properties (Chiorini *et al*., 1999;

[1]Department of Chemical Engineering and Helen Wills Neuroscience Institute, University of California, Berkeley, CA 94720.
[2]Howard P. Isermann Department of Chemical and Biological Engineering, Rensselaer Polytechnic Institute, Troy, NY 12180.

Gao *et al*., 2004). AAV2 remains the most widely used to date, because of its extensive safety record and well-characterized gene delivery properties. In addition, recombinant (r)AAV2 vectors have been explored in numerous clinical trials (Kay *et al*., 2000; Manno *et al*., 2003). However, other serotypes have also shown substantial progress (Sarkar *et al*., 2006).

One challenge with rAAV vectors involves the development of a scalable, high-throughput purification protocol that can be generally applicable to all serotypes. The original purification scheme employed a virus precipitation followed by two or three rounds of ultracentrifugation through an isopycnic cesium chloride (CsCl) gradient, which also often resulted in low recovery and limited throughput and scalability (Snyder, 1996). Advances in AAV purification have focused on enhancing viral recovery while retaining its biological activity through chromatographic methods, such as affinity and ion exchange. In particular, affinity chromatography has successfully allowed for rapid purification of AAV2 through columns packed with either a monoclonal antibody that recognizes a conformational epitope on the viral capsid (Grimm *et al*., 1998) or heparin, structurally similar to the heparan sulfate proteoglycan (HSPG) primary receptor for AAV2 (Clark *et al*., 1999; Zolotukhin *et al*., 1999; Auricchio *et al*., 2001). Heparin affinity resins have been used to isolate high-titer rAAV2 stocks directly from clarified cell lysate at yields ranging from 30 to 75%, with few protein contaminants. Unfortunately, most novel AAV serotypes cannot bind existing affinity resins based on heparin or sialic acid (Walters *et al*., 2001), creating the need for serotype-specific resins. By comparison, ion exchange is broadly applicable for the purification of multiple AAV serotypes, but it requires reoptimization of buffer conditions for each serotype (Brument *et al*., 2002; Kaludov *et al*., 2002). As an alternative, Bartlett and coworkers have employed an avidin affinity column platform to successfully purify multiple AAV serotypes into which a biotin acceptor peptide (BAP) was engineered, although purification required use of a density gradient separation before column application (Arnold *et al*., 2006). It would be advantageous to generate a rapid, robust purification method that combines the single-step efficacy of affinity resins with the generality of ion exchange.

Genetic modification of AAV has allowed for the study and design of its gene delivery properties. For example, mutagenesis studies have elucidated amino acids critical for heparan sulfate binding (Kern *et al*., 2003; Opie *et al*., 2003) as well as other regions required for infectivity (Rabinowitz *et al*., 1999; Wu *et al*., 2000; Shi *et al*., 2001). In addition, numerous efforts to alter viral tropism, along with the elucidation of the AAV2 crystal structure (Xie *et al*., 2002), have led to the identification of several regions in the AAV2 capsid amenable to peptide insertions, and an increasing number of studies have introduced peptides into other AAV serotypes (Girod *et al*., 1999; Grifman *et al*., 2001; Shi *et al*., 2001; Muller *et al*., 2003; Perabo *et al*., 2003). However, some peptide insertions drastically reduce viral production titers or viral infectivity, whereas others may not be functionally displayed on the capsid surface. Also, different peptide sequences inserted into the same location in the capsid may not be functionally displayed equally, and subtle differences in the sequences of flanking amino acids can yield variants with infectivities differing by several orders of magnitude (Wu *et al*., 2000; Shi *et al*., 2001). Transposon-based saturation mutagenesis approaches have proven useful for mapping novel insertion sites with viral genomes and proteins (Brune *et al*., 1999; Yu and Schaffer, 2006). We therefore employed a dual approach in which an affinity purification tag was rationally inserted at several sites, and an insertional mutagenesis library was generated and explored for other potentially permissive sites.

Immobilized metal affinity chromatography (IMAC) has broad applicability in the area of protein purification because of low cost, high loading capacity, minimal product loss, and mild solution conditions. For example, hexahistidine (His_6) tags bind reversibly with micromolar affinity to nickel nitrilotriacetic acid (Ni-NTA) (Porath *et al*., 1975; Kapanidis *et al*., 2001) and have been employed to purify several viral vectors via IMAC with various degrees of success (Hu *et al*., 2003; Ye *et al*., 2004; Yu and Schaffer, 2006). Previous insertion of a flexible linker followed by a His_6 tag at the end of the AAV2 VP3 capsid protein generated infectious AAV particles with the ability to bind Ni-NTA beads (Zhang *et al*., 2002). However, important results (such as purity and yield) were not reported. In a separate study, insertion of a His_6 tag severely decreased viral production levels and abolished viral infectivity (Wu *et al*., 2000).

We have successfully generated two novel His_6-containing AAV mutants, based on AAV2 and the first reported AAV8 peptide insertion, that generate high-titer rAAV vector readily and effectively purified via single-step, gravity Ni-NTA column chromatography for application *in vitro* and *in vivo*. Furthermore, the combined rational insertion and library-based approach may allow for the identification of optimal insertion sites for specific peptides in the capsid of any AAV serotype, thereby improving the process of viral vector design and application.

MATERIALS AND METHODS

Construction of AAV plasmids

To construct pXX2Not, a 1.8-kilobase linear fragment containing a portion of the backbone sequence of pXX2 (Xiao *et al*., 1998) was generated by polymerase chain reaction (PCR), using the primers 5′-GCGAAGCTTACGCGGCCGCTTGTTAATCAATAAACCGTTTAATTCG-3′ and 5′-CGGAATGGACGATATCCCGC-3′ with pXX2 (Xiao *et al*., 1998) as template. Both this product and pXX2 were digested with *Hin*dIII and *Cla*I, and the products were ligated to create the rAAV packaging plasmid pXX2Not. The *cap* sequence from AAV8 was cloned into this vector as well. To construct each peptide mutant, spliced overlap extension PCR was used to insert the His_6 peptide epitopes into the correct location, sometimes with additional flanking sequences (primer sequences and cloning details are available on request). In addition, an AAV2 library containing a randomly inserted His_6 sequence within the *cap* gene was packaged (Maheshri *et al*., 2006) and selected as previously described (Yu and Schaffer, 2006). Briefly, the chloramphenicol resistance (Cam^R) gene was randomly inserted into a plasmid containing the AAV2 *cap* gene, using a transposon kit (Finnzymes, Espoo, Finland). The resulting plasmid library was digested to excise the *cap*-Cam^R genes, which were subsequently cloned into pSub2 (Maheshri *et al*., 2006). The pSub2 plasmid library was digested with *Not*I before ligation to His_6

fragments phosphorylated with T4 polynucleotide kinase. The His_6 insert was constructed with the following oligonucleotides, with the histidine codons shown in boldface: 5′-GGCCGGT-**CACCACCACCACCACCAC**TC-3′ and 5′-GGCCGA**GTG-GTGGTGGTGGTGGTG**ACC-3′.

Cell lines and vector production

HEK293T, HeLa, CHO K1, CHO pgsA, and CHO pgsD were cultured in Iscove's modified Dulbecco's medium (IMDM; Mediatech, Herndon, VA) with 10% fetal bovine serum (Invitrogen, Carlsbad, CA) and 1% penicillin and streptomycin (Invitrogen) at 37°C and 5% CO_2. All cell lines were obtained from the American Type Culture Collection (ATCC, Manassas, VA). AAV293 cells (Stratagene, La Jolla, CA) were cultured in Dulbecco's modified medium (DMEM) with 10% fetal bovine serum and 1% penicillin and streptomycin at 37°C and 5% CO_2.

rAAV was produced as previously described (Kaspar *et al*., 2003; Maheshri *et al*., 2006). Briefly, in a 15-cm plate of ~80% confluent AAV293 cells (Stratagene), ~15 μg of pAAV CMV-GFP, 15 μg of pHelper (Stratagene), and 15 μg of one of the modified pXX2Not plasmids were transfected by the calcium phosphate method. Viral vectors were harvested as previously described (Maheshri *et al*., 2006). Vector packaged in wild-type capsid was purified via an iodixanol gradient followed by heparin column chromatography (Zolotukhin *et al*., 1999). DNase-resistant genomic titers were determined by quantitative PCR, and infectious titers were determined by flow cytometry as previously described (Maheshri *et al*., 2006).

Ni-NTA purification of viral vectors

A mixture of 1 volume of cell lysate containing virus, 0.5 volume of binding buffer (10 m*M* Tris [pH 8.0], 300 m*M* NaCl, and 20 m*M* imidazole), and 500 μl of 50% Ni-NTA agarose (Qiagen, Valencia, CA) was agitated gently overnight at 4°C. This mixture was then loaded onto a plastic column (Kontes, Vineland, NJ) before washing with 5 ml of wash buffer (10 m*M* Tris [pH 8.0], 50 m*M* imidazole) and eluting with 2–3 ml of elution buffer (10 m*M* Tris [pH 8.0], 500 m*M* imidazole). Finally, the eluted virus was buffer exchanged into Tris-buffered saline (TBS) and concentrated with Microcon spin columns (Millipore, Billerica, MA) according to the manufacturer's instructions.

Equivalent amounts of each column sample from a large-scale purification scheme were separated by sodium dodecyl sulfate–polyacrylamide gel electrophoresis (SDS–PAGE). Proteins were detected with a silver stain kit (Bio-Rad, Hercules, CA). The DMEM and viral cell lysate samples analyzed on the same gel were diluted 1:10 to prevent oversaturation of the silver stain signal.

For Western blot analysis, equivalent amounts of green fluorescent protein (GFP) vector packaged with wild-type AAV2 and His_6 capsids were separated by sodium dodecyl sulfate–polyacrylamide gel electrophoresis and transferred to a nitrocellulose blot. The blot was blocked in Tris-buffered saline with 3% bovine serum albumin and incubated with penta-His antibody (Qiagen) according to the manufacturer's instructions. The blots were then developed by enhanced chemiluminescence (ECL) detection assay (GE Healthcare Life Sciences, Piscataway, NJ).

In vitro *characterization of viral vectors*

To assay for heparin binding, ~10^{11} purified genomic particles of virus were loaded onto a 1-ml HiTrap heparin column (GE Healthcare Life Sciences) previously equilibrated with 150 m*M* NaCl and 50 m*M* Tris at pH 7.5. The virus was eluted with 0.75-ml volumes of 50 m*M* Tris buffer containing increasing increments of 50 m*M* NaCl up to 750 m*M*, followed by two 1 *M* washes. To quantify the amount of infectious virus present in each fraction, 75 μl of each elution fraction was added to 2.5×10^5 293 cells in 12-well format. At 48 hr postinfection, the fraction of green cells was quantified by flow cytometry (EPICS; Beckman Coulter, Fullerton, CA) at the Berkeley Cancer Research Laboratory (University of California, Berkeley, CA).

To compare cell tropism, either wild-type or mutant rAAV-GFP particles were added to 293T, HeLa, CHO K1, CHO pgsA, and CHO pgsD cell lines at a genomic multiplicity of infection (MOI) of 1000. After 48 hr, the fraction of green cells was quantified by flow cytometry (EPICS) at the Berkeley Cancer Research Laboratory. Antibody neutralization assays using human intravenous immunoglobulin (IVIG; Bayer Biological Products, Research Triangle Park, NC) were performed as previously described (Maheshri *et al*., 2006).

Animal surgeries and histology

Recombinant AAV vectors were stereotaxically injected into the striatal region of the brain (anteroposterior [AP], +0.2; mediolateral [ML], ±3.5; dorsoventral [DV], –4.5 from skull) of adult female Fischer 344 rats (150 g, 6 weeks old). The animals were deeply anesthetized with a mixture of ketamine (90 mg/kg) and xylazine (10 mg/kg) before injection, and 3 μl of high-titer AAV vector (1×10^9 vector genomes [VG]/μl) was injected with a Hamilton syringe. Animals were transcardially perfused with 4% paraformaldehyde (PFA) in phosphate-buffered saline (PBS), and the brains were excised either 3 days or 3 weeks postinjection, to detect immune responses ($n = 2$ per condition) or to quantify GFP expression ($n = 3$ per condition), respectively. The retrieved brains were postfixed by immersion in 4% PFA overnight at 4°C and subsequently stored in 30% sucrose for cryoprotection before sectioning.

Coronal sections (thickness, 40 μm) were cut with a freezing, sliding microtome. Primary mouse anti-macrophages/monocytes (clone ED-1, diluted 1:100; Chemicon International, Temecula, CA) and mouse anti-CD8 α chain (clone OX-8, diluted 1:100; Chemicon International) were used to detect antigens expressed by macrophages and T cells, respectively. In addition, primary mouse anti-neuron-specific nuclear protein (NeuN, diluted 1:200; Chemicon International) and guinea pig anti-glial fibrillary acidic protein (GFAP, diluted 1:1000; Advanced ImmunoChemical, Long Beach, CA) were used to identify cell types (i.e., neurons and glial cells), and GFP expression was amplified with primary rabbit anti-GFP (diluted 1:2000; Invitrogen). Corresponding secondary antibodies (labeled with Alexa Fluor 488, 546, and 633) were used for detection. For nuclear staining, some sections were counterstained with TO-PRO-3 (diluted 1:2000; Invitrogen). The sections containing regions exhibiting GFP expression were collected, and the total volume of GFP expression was quantified by a modified stereology method (Yu and Schaffer, 2006). Statistical comparisons between wild-type AAV and His_6 AAV injections

were performed with the analysis of variance (ANOVA) *t* test (JMP software; SAS Institute, Cary, NC). Animal protocols were approved by the University of California, Berkeley (UCB) Animal Care and Use Committee and conducted in accordance with National Institutes of Health (NIH, Bethesda, MD) guidelines.

RESULTS

Construction of AAV mutants containing His_6 tag

We constructed a library of *cap*-Cam^R insertion mutants, using a MuA transposase and a modified transposon insert containing a chloramphenicol resistance gene (Cam^R). The resulting *cap*-CAM^R library was cloned into the AAV vector pSub2, and the Cam^R gene was subsequently replaced with a His_6-encoding insert to create the final library. Five nucleotides from *cap* become duplicated at the insertion site during the transposition reaction, and these together with the His_6 sequence yield a 13-amino acid insertion. Restriction digest analysis of individual clones from the library confirmed that the insertions occurred throughout the entire *cap* gene and that each of these clones contained only one insert (data not shown). The estimated diversity of the library was $\sim 5 \times 10^4$ independent insertions into the 2.6-kb *cap* PCR product, which thus likely provides full coverage of all possible insertion sites. The library was significantly diluted and used to package replication-competent AAV (rcAAV), as we have previously described for AAV library packaging (Maheshri *et al*., 2006).

Although the library likely contains every insertion site, the flanking residues for the His_6 tag, which consist of four alanine residues along with three random amino acids, may decrease infectivity because of the large insertion size or may not be optimal for display of the His_6 tag. Therefore, in parallel, we constructed a series of defined *cap*-His_6 insertion mutants by spliced overlap extension PCR. These AAV2 insertion sites, previously shown to be permissive to the insertion of peptide sequences, were located in three regions: immediately after amino acid position 584 (Shi *et al*., 2001), after amino acid position 587 (Girod *et al*., 1999), and after amino acid position 588 (Grifman *et al*., 2001) (Fig. 1A). In addition, an AAV8 mu-

A

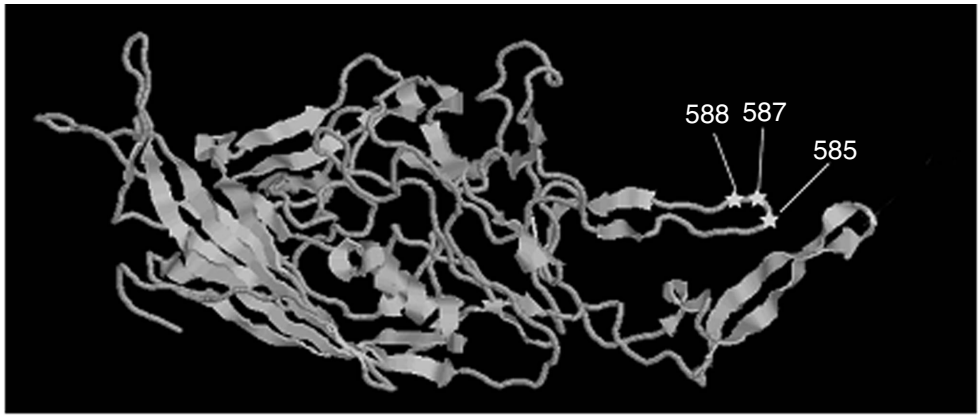

B

Location	Amino Acid Sequence
WT AAV2	~^{583}LQRGNRQA~
His584	~LQ*LG***HHHHHHH***S*RGNRQA~
His587	~LQRGN*LG***HHHHHHH***S*RQA~
His588	~LQRGNR*LG***HHHHHHH***S*QA~
HisAAV8	~QQQN*LG***HHHHHHH***S*TAP~

FIG. 1. Design of His_6 AAV mutants. (**A**) Map of VP3 monomer, constructed with Rasmol, indicating where insertions of His_6 tag occurred. (**B**) Sequences of wild-type AAV2 compared with each of the His_6 AAV2 clones, along with the His_6 AAV8 clone. His_6 tags are shown in boldface and flanking residues are shown in italics.

tant containing the peptide insertion in an analogous loop, after amino acid position 590, was constructed. Each insert contained a His_6 sequence flanked by leucine and glycine on the N-terminal side and serine on the other to aid in efficient peptide display (Fig. 1B). These mutant *cap* variants were inserted into a modified AAV helper plasmid, pXX2Not, based on pXX2 (Xiao *et al*., 1998).

Analysis of packaging and Ni-NTA-binding ability of AAV clones

To select the *cap*-His_6 random insertion library for variants capable of binding to Ni-NTA resin, while retaining viral infectivity, the viral library was passed through an Ni-NTA column. The virus present in the elution fractions was then amplified at a low MOI in 293T cells, followed by the addition of adenovirus serotype 5 (Ad5) to induce replication of the infectious AAV variants, which were again applied to the Ni-NTA column. After only two such rounds of selection, sequence analysis of the library indicated that the pool contained one dominant clone with an insertion after amino acid position 454, which bound to the Ni-NTA column at levels greatly exceeding that of wild-type AAV2 (data not shown). The resulting His_6-*cap* gene, along with a corresponding His_6-*cap* gene in which the His_6 tag was rationally inserted at position 454 with the same leucine, glycine, and serine flanking amino acids used in the other defined insertion clones, were then inserted into pXX2Not. These constructs along with the other rationally designed His_6 clones were then used to package rAAV-GFP.

Initial characterization of both the library-derived His_6-AAV clone and rationally designed His_6-AAV variants indicated, surprisingly, that only one (His-587) produced high-titer, infectious virus ($>10^5$ IU/ml). Initial, small-scale production on a 10-cm plate yielded $\sim 4 \times 10^6$ IU/ml in clarified cell lysate for this His_6 mutant, compared with $\sim 3 \times 10^7$ IU/ml for wild-type AAV2 capsid. The remaining AAV2 clones, including the variant with the insertion at amino acid 454 identified from the viral library, packaged virus with poor infectivity, that is, with genome:infectious ratios of $>10^5$ (data not shown). Optimization of the transposition reaction, which incorporates an additional five amino acids onto each peptide insertion, may require the use of alternative transposases or extensive mutagenesis work to remove the extraneous nucleotides or the addition of several rounds of amplification before selection, despite the fact that the analogous approach worked effectively in the generation of His-tagged vesicular stomatitis virus protein for retroviral and lentiviral purification (Yu and Schaffer, 2006). It is possible that the need for viral proteins to assemble into a 60-mer capsid, rather than a trimer envelope protein, places additional constraints on the insert location and sequence.

Importantly, the AAV2 variant with a His_6 tag inserted after amino acid 587 (His_6 AAV2), when applied to the Ni-NTA column in clarified cell lysate, bound at levels vastly exceeding that of wild-type AAV2 (Fig. 2A and B). Further optimization of incubation times, buffer pH, wash conditions, and elution conditions, using the His_6 AAV2 clone, resulted in a total infectious virus recovery exceeding 90% in a relatively small volume (~1–2 ml). Interestingly, only a moderate 10% of the total DNase-resistant AAV2 viral genomes were recovered from the column, indicating the presence of a large population of noninfectious, DNase-resistant genomes in the crude lysate that were unable to bind to the column. This result is consistent with prior peptide insertions into this region of the AAV2 capsid (Wu *et al*., 2000; Shi *et al*., 2001).

In parallel, the His_6 AAV8 variant, containing an identical peptide insertion after amino acid 590, showed no significant difference in viral production levels. Remarkably, on application of His_6 AAV8 to the Ni-NTA column, more than 90% of both the DNase-resistant viral genomes and infectious virions were recovered from the column (Fig. 2A and B), in marked contrast to the His_6 AAV2 results.

We scaled up the purification and generated high-titer rAAV2-GFP by the direct application of clarified crude lysate to a column packed with Ni-NTA resin and elution of the bound virus with high concentrations of imidazole. We also generated high-titer rAAV2-GFP with the wild-type AAV2 capsid by a conventional two-step purification procedure (i.e., centrifugation through an iodixanol gradient followed by flow through a heparin column) (Zolotukhin *et al*., 1999). To assess viral purity, SDS–PAGE analysis followed by silver staining was conducted on the IMAC column-purified virus compared with conventional iodixanol and heparin column-purified rAAV2-GFP (Zolotukhin *et al*., 1999). The result indicated a negligible difference between the purities of the final viral stocks (Fig. 2C, lane 5 vs. lane 9 in the intentionally overdeveloped silver-stained gel), and Western blot analysis confirmed the presence of the His_6 tag within all three viral capsid proteins (Fig. 2D).

In vitro *characterization of His_6-tagged AAV*

Because the His_6 insertion occurs within a region of the AAV2 capsid important for heparan sulfate binding (Kern *et al*., 2003; Opie *et al*., 2003), we further analyzed the properties of His_6 AAV2 *in vitro*. Both purified His_6 AAV2 and vector packaged in wild-type capsid were loaded onto a heparin column and eluted with a series of increasing salt concentrations, and infectious viral titers within each fraction were determined by flow cytometry. Wild-type AAV2 eluted in a sharp peak from 400 to 500 m*M* NaCl, consistent with previous reports (Clark *et al*., 1999; Maheshri *et al*., 2006), whereas His_6 AAV2 eluted in a broad range, beginning at 200 m*M* NaCl and followed by a long tail stretching to 750 m*M* NaCl, indicating a mixed population of infectious virions with variable heparin affinities (Fig. 3A).

In addition, several cell lines possessing various levels of heparan sulfate were employed to analyze the cell tropism of the mutant relative to wild-type AAV2 (Fig. 3B). Infection of 293T and HeLa cell lines showed a modest 2- to 4-fold reduction in the ratio of infectious to genome titers of His_6 AAV2, respectively, compared with wild-type AAV2. However, this difference increased to almost 10-fold on the native CHO K1 cell line and two mutant cell lines, CHO pgsA and pgsD, defective in HSPG biosynthesis (Esko *et al*., 1985), indicating that the mutant was more sensitive to lower HSPG levels, likely because of disruption of the heparan sulfate-binding region on the viral capsid. Previous reports from ourselves and others indicated that peptide insertion or a single point mutation within this region conferred moderate resistance to antibody neutralization (Huttner *et al*., 2003; Maheshri *et al*., 2006). Consistent

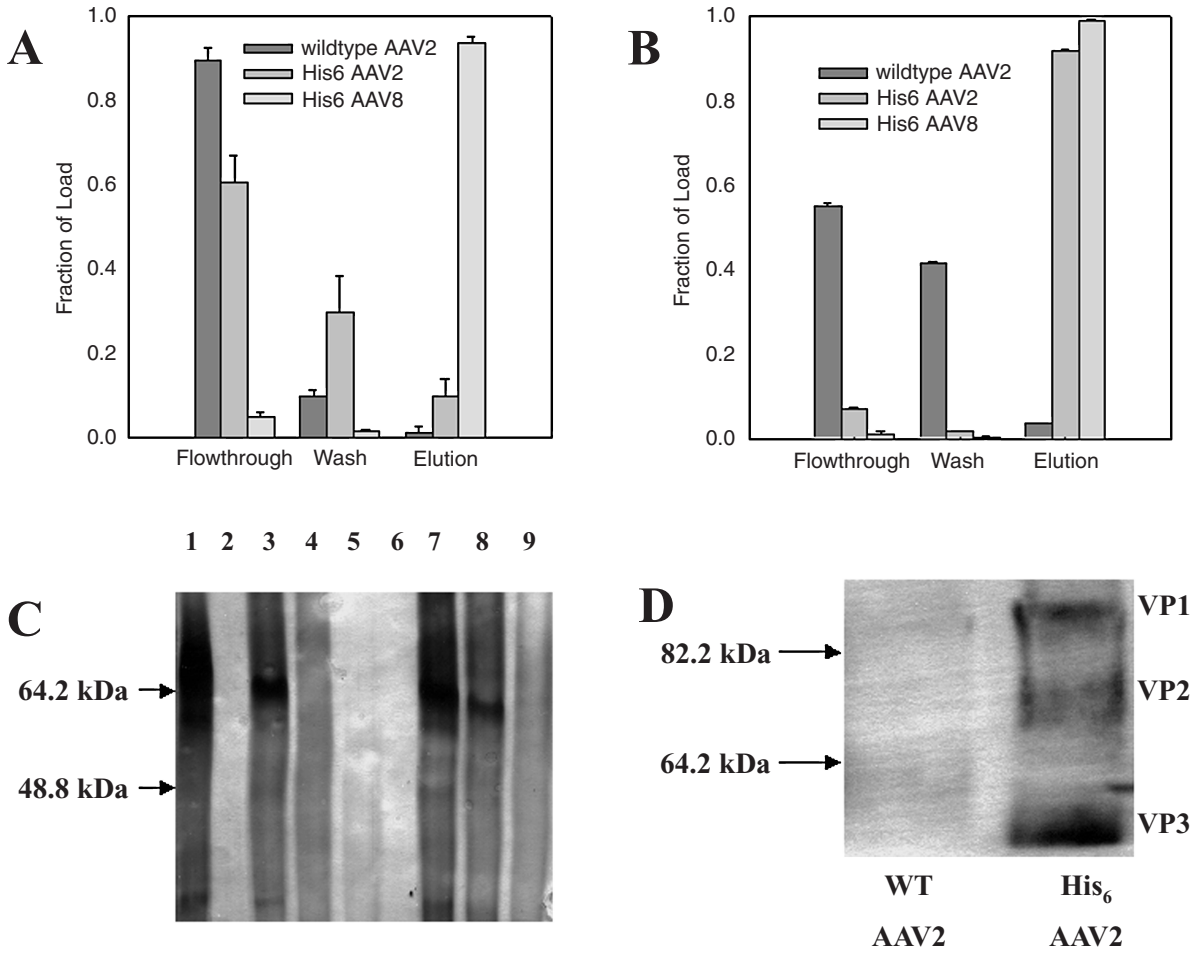

FIG. 2. Ni-NTA purification of His_6 AAV mutant. (**A**) Representative genomic titers of recombinant GFP vector packaged inside wild-type AAV2 capsid, His_6 AAV2, and His_6 AAV8 present within each column fraction. Titers were determined by quantitative PCR, and error bars represent the standard deviation of three independent trials. (**B**) Representative transduction titers of recombinant GFP vector packaged with wild-type AAV2 capsid, His_6 AAV2, and His_6 AAV8 present within each column fraction. Titers were determined by flow cytometry, and error bars represent the standard deviation of three independent trials. (**C**) Silver stain analysis of His_6 AAV, purified via Ni-NTA, and of wild-type AAV2, purified via iodixanol and heparin affinity chromatography. Lane 1, DMEM with 10% fetal bovine serum (1:10 dilution); lane 2, blank; lane 3, Ni-NTA column flowthrough (1:10 dilution); lane 4, column wash; lane 5, column elution; lane 6, blank; lane 7, clarified viral cell lysate (1:10 dilution); lane 8, iodixanol purified wild-type AAV2; lane 9, iodixanol and heparin column-purified wild-type AAV2. The protein gel was intentionally overexposed to detect minor quantities of protein contaminants within each sample. (**D**) Western blot detection of His_6 tag within AAV capsid proteins, using a penta-His antibody.

with these findings, the His_6 insertion conferred to the viral vector a ~6-fold improvement in gene delivery relative to wild-type AAV2 in the presence of pooled intravenous human immunoglobulin (IVIG) (Fig. 3C).

In vivo *performance of AAV vectors*

Vector purification methods should yield viral vectors with high *in vivo* biological activity, while minimizing any immunogenic response arising from contaminants. IMAC-purified His_6 AAV2 and iodixanol/heparin column-purified AAV2 (1×10^9 DNase-resistant particles/μl), carrying cDNA encoding GFP driven from a human cytomegalovirus (CMV) promoter, were stereotactically injected into the rat striatum. Two weeks postinjection, robust GFP expression was observed in all animals, and the cellular tropism of His_6 AAV2 remained identical to that of vector packaged with wild-type capsid, with infection primarily of cells staining positive for the neuronal marker NeuN, with minimal apparent infection of cells expressing the astrocytic marker GFAP (Fig. 4A and B). Interestingly, a small number of neurons exhibited GFP expression adjacent to the needle track only 3 days after injection of both vectors (data not shown). In addition, there was no statistically significant difference in viral infection spread along the anterior–posterior axis or the total volume accessed by viral vector infection between the two viral preparations (Fig. 4C and D), indicating that the His_6 AAV2 variant is highly efficient *in vivo* and that its performance is not substantially affected by altered heparin affinity. A potential concern for gene therapy is the development of a host immune response against the injected vi-

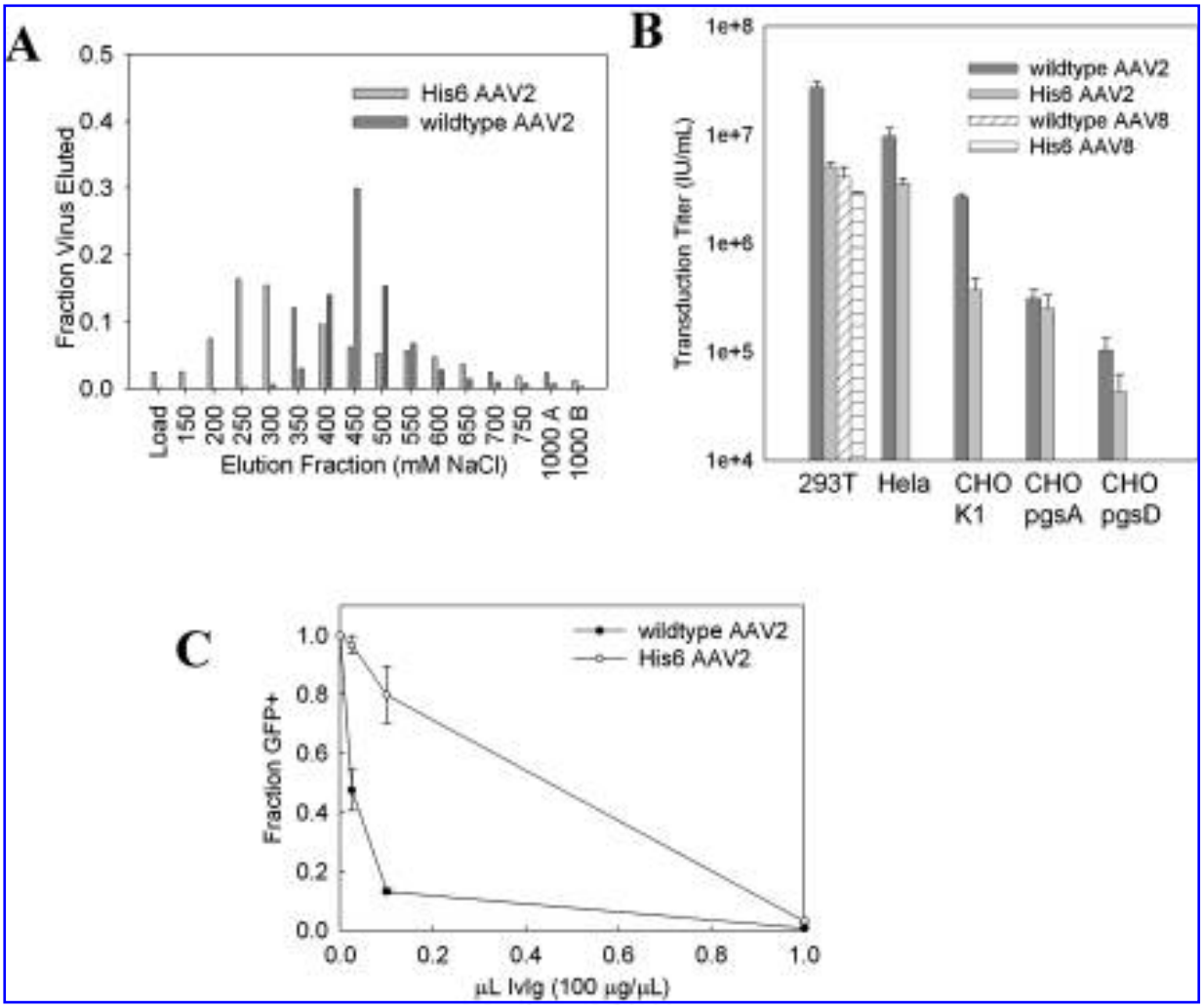

FIG. 3. *In vitro* characterization of His_6 AAV gene delivery properties. (**A**) Heparin column chromatograms for wild-type AAV2 and His_6 AAV2. (**B**) Representative transduction titers of recombinant GFP vector packaged by wild-type AAV2 and His_6 AAV2 on several cell lines expressing various levels of HSPG, and representative transduction titers of wild-type AAV8 and His_6 AAV8 on 293T cells. Error bars represent the standard deviation of studies performed in triplicate. (**C**) Relative gene delivery efficiency of wild-type AAV2 and His_6 AAV2 in the presence of various amounts of human intravenous immunoglobulin. Error bars represent the standard deviation of studies performed in triplicate.

ral vector (Manno *et al*., 2006). Three days postinjection, minimal activation of either CD8-positive T lymphocytes or macrophages was observed with either viral vector (Fig. 4E and F). Control injections with PBS exhibited similar low activation levels of macrophages and few CD8-positive T lymphocytes (data not shown).

DISCUSSION

Column chromatography-based viral vector purification offers high vector yields and throughput with low levels of contaminants compared with conventional density gradient purifications. Column platforms based on either affinity- or ion-exchange chromatography have successfully permitted rapid, efficient purification of multiple AAV serotypes (Grimm *et al*., 1998; Clark *et al*., 1999; Zolotukhin *et al*., 1999; Auricchio *et al*., 2001; Walters *et al*., 2001; Brument *et al*., 2002; Kaludov *et al*., 2002); however, the variable capsid properties of each serotype force novel affinity systems or purification conditions to be continuously redesigned. Advances in genetic engineering permit the customized design of AAV vectors for improved gene delivery, often based on insertion of exogenous peptide sequences into the viral capsid (Muller *et al*., 2003; Perabo *et al*., 2003; Maheshri *et al*., 2006). However, significant challenges, such as the design of proper flanking sequences or the location of alternate insertion sites, can hinder the use of rational design to identify optimal insertion sites or amino acids critical for the novel vector property. In addition, the local protein environment strongly affects the functional display of a foreign peptide, and a single amino acid change in its sequence may dramatically reduce vector production or infectivity (Wu *et al*., 2000; Shi *et al*., 2001). Joint application of rationally designed AAV capsids and a combinatorial library of capsid variants,

created via the random insertion capabilities of transposases, may assist in the rapid design of customized viral gene delivery vectors.

Here, we have constructed a large *cap*-His_6 insertion library likely containing variants with insertions at every internucleotide site of the entire AAV2 *cap* gene. In parallel, we generated rational AAV *cap*-His_6 mutants based on locations previously shown to be amenable to foreign peptide insertion (Girod *et al*., 1999; Grifman *et al*., 2001; Shi *et al*., 2001). Subsequent, iterative rounds of library selection over immobilized metal resin and amplification in 293T cells resulted in the isolation of a dominant, Ni-NTA binding AAV2 mutant. Upon characterization of the viral production ability of both this dominant His_6 AAV mutant and the rational insertions, however, we found that only one mutant, with an insertion after amino acid site 587, was capable of efficiently packaging high-titer rAAV2. In addition, an AAV8 mutant with an insertion in the analogous region of the capsid (after amino acid site 590) was capable of packaging high-titer rAAV, representing to our knowledge the first peptide insertion into the AAV8 capsid. The extension of the (His_6) insertion to AAV8 enhances the utility of the approach, as AAV8 has been shown to be highly efficient in delivery to hepatocytes, skeletal and cardiac muscle, and dopaminergic neurons (Conlon *et al*., 2005; Wang *et al*., 2005; Klein *et al*., 2006). For AAV2, interestingly, the shift of the insertion site by one amino acid from amino acid 587 to amino acid 588, drastically reduced viral infectivity, highlighting the crucial importance of insert location and flanking sequences for optimal function of a peptide insert. Surprisingly, the dominant clone identified from the high-throughput library selection, with the insert located after amino acid 454, bound Ni-NTA resin, but failed to yield infectious virus and was thus not further pursued.

The loop III and loop IV regions within the AAV capsid have been used for peptide insertions with various degrees of success. The loop III region is located at the apex of the 3-fold proximal peaks on the capsid (Xie *et al*., 2002), and deletion of this region has been shown to result in a >20-fold reduction in viral infectivity (Grifman *et al*., 2001). A variety of peptide insertions within this region have been performed with various degrees of success. Insertion of some peptides such as L14 (containing the RGD motif of laminin fragment P1) (Girod *et al*., 1999), NGR (Grifman *et al*., 2001), and hemagglutinin (HA) (Wu *et al*., 2000) resulted in infectious virus with a functionally displayed peptide epitope, whereas insertion of other peptides such as luteinizing hormone (LH) (Shi *et al*., 2001) and serpin (Wu *et al*., 2000) abolished viral infectivity. On the other hand, the other insertion sites studied occur within the well-studied loop IV (amino acids 583–590) of the AAV capsid. In the case of AAV2, this region is crucial for HSPG binding, and peptide insertions that decrease HSPG binding correlate with at least 100- to 1000-fold decreases in viral infectivity (Girod *et al*., 1999; Grifman *et al*., 2001; Shi *et al*., 2001), whereas peptide insertions within analogous regions of several alternative AAV serotypes have been well tolerated with no drastic reduction in viral infectivity (Arnold *et al*., 2006). These results suggest that although this region (loop IV) provides an optimal location for efficient peptide display within multiple AAV serotypes, peptide insertions into this region have the potential to disrupt structural motifs crucial for the native viral tropism or other biological functions. The results of previous studies, together with the His_6 mutants described above, therefore highlight the need to customize both flanking amino acids and insertion site for each novel peptide, especially for retargeting applications.

Protein engineering techniques in general have the potential to aid in the development of a rapid, robust purification platform for viral vectors. A previous study generated an AAV2 mutant containing a His_6 tag along with a flexible linker at the carboxyl terminus of VP3 through simultaneous transfection of the viral genes for VP1–VP2 and VP3 under the control of the nonnative CMV promoter (Zhang *et al*., 2002). Although successful purification of rAAV vectors via Ni-NTA column chromatography was reported, important quantitative parameters such as purity and yield were not included, nor were purified vectors analyzed for efficient *in vivo* delivery efficiency (Wu *et al*., 2000). Thus, a novel insertion site for a His_6 tag in the AAV capsid for the production of high-titer rAAV offers advantages. This study identifies such an insertion site within multiple AAV serotypes and extends the use of high-yield and extremely pure His_6 AAV2, purified via a Ni-NTA column, for gene delivery to the central nervous system with no appreciable host immune response. One study demonstrated that the successful insertion of a biotin acceptor peptide into several locations of multiple AAV serotypes facilitated novel AAV vector purification via a monomeric avidin column (Arnold *et al*., 2006). The yields and purity of vectors of several serotypes were promising, although an initial fractionation step via ultracentrifugation in an iodixanol gradient was necessary to remove biotinylated cellular proteins and free biotin. Also, the extremely high affinity between biotin and even monomeric avidin resulted in viral retention on the column (Parrott *et al*., 2003), whereas metal-binding tags can offer a moderate-affinity, reversible linkage with immobilized metal columns.

These novel His_6 AAV2 and AAV8 mutants facilitated rapid, robust purification of >90% recovery of infectious rAAV within clarified crude lysate, which compares well with previous affinity- and ion-exchange chromatography methods. The AAV2 variant capable of producing high-titer virus contained the His_6 tag within a region (amino acids 585–588) that facilitates HSPG binding (Kern *et al*., 2003; Opie *et al*., 2003) and therefore may alter the natural tropism of the virus. The heparin column chromatogram indicates that the infectious viral particles contain a range of affinities for heparin, with the majority exhibiting a lower affinity that could allow for improved transport through extracellular matrix regions in tissues that contain high levels of HSPG (Fig. 3A). Although the reduction in heparin affinity associated with a peptide insertion within this region has been reported (Wu *et al*., 2000; Shi *et al*., 2001), we hypothesize that the presence of a fraction of virus with wild-type or apparently even higher heparin affinity could be due in part to the inherent affinity of His_6 tags for heparin (Lacy and Sanderson, 2002). However, the broad range of heparin affinities suggests other factors such as salt concentration may alter the pK_a of histidine (Lee *et al*., 2002) and hence alter the degree of protonation within the heparan sulfate-binding region. Furthermore, the observed reduced infectivity on several CHO cell lines (Fig. 3B) defective in HSPG biosynthesis advances the idea that overall this vector is more sensitive to cell surface levels of HSPG, although this sensitivity did not compromise *in vivo* delivery. These results agree with our previous study in

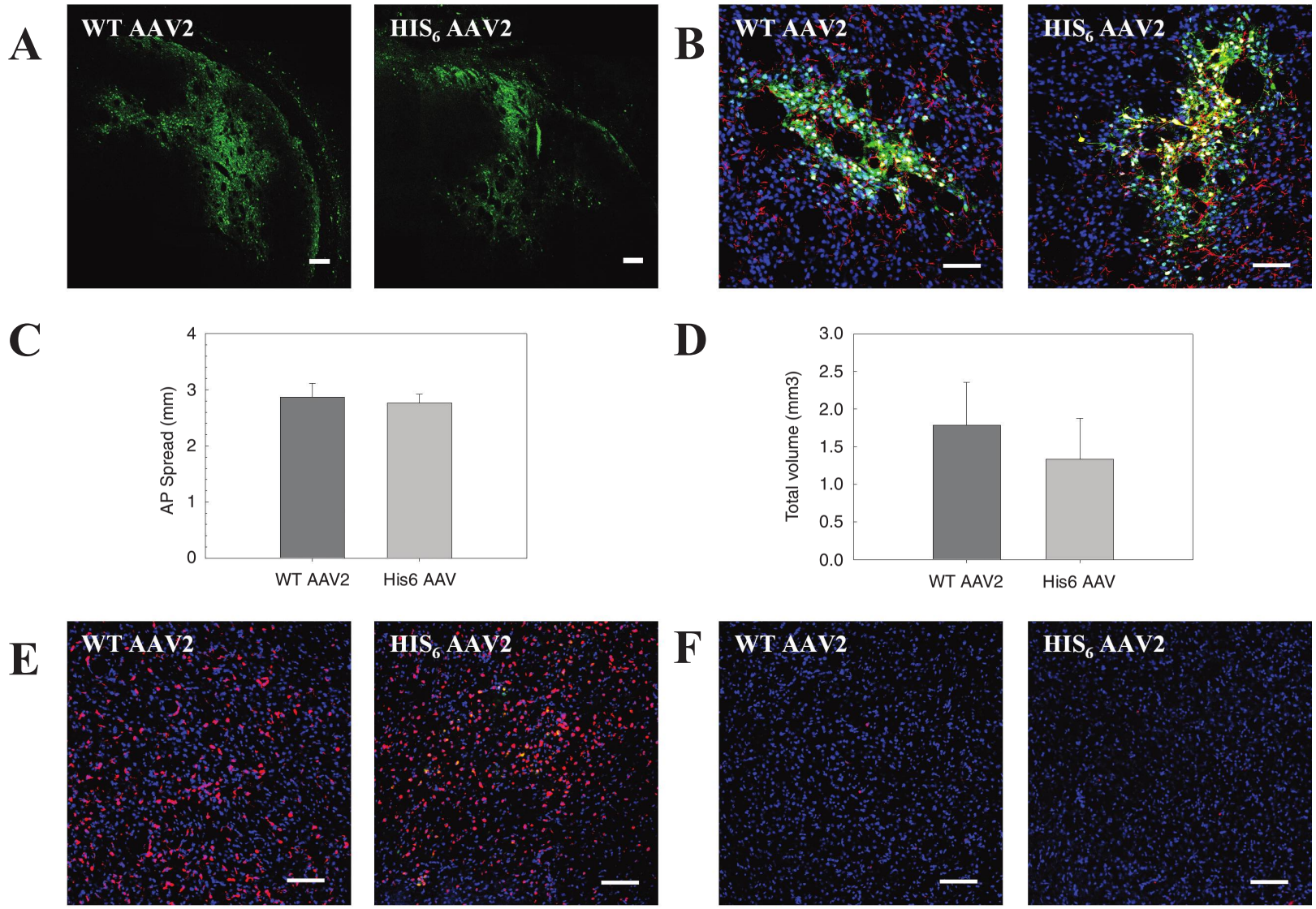

FIG. 4. *In vivo* comparisons between injections of GFP-expressing vectors with either wild-type AAV2 or His_6 AAV2 capsid: GFP expression after 3 weeks (**A**–**D**), immune responses after 3 days (**E** and **F**). (**A**) Representative images of infections with either wild-type AAV2 or His_6 AAV2 within the rat striatum show similar levels of GFP expression (green) at 3 weeks postinjection. For (**A**), multiple panels (10× objective) were assembled to represent the entire GFP-expressing region. (**B**) Representative images of cell types residing adjacent to GFP-expressing cells demonstrate the equivalent tropism for wild-type AAV2 and His_6 AAV2 (20× objective): $NeuN^+$ neurons (blue), $GFAP^+$ astrocytes (red), and GFP^+ cells (green). (**C**) The anterior–posterior (AP) spread of GFP expression indicates no significant difference between the two vectors ($p > 0.05$). The AP spread was the distance between the first and last tissue sections exhibiting GFP expression. (**D**) The total volume of GFP expression ($p > 0.05$). The error bars for (**C**) and (**D**) indicate the standard deviations. (**E** and **F**) Macrophage ($ED\text{-}1^+$, red) and T cell ($OX\text{-}8^+$, red) migration toward the injection sites, respectively. Nuclei were counterstained with TO-PRO-3 (blue). (**E**) and (**F**) represent regions approximately 200 μm away from the injection sites. Scale bars (**A**, **B**, **E**, and **F**): 200 μm.

which an AAV2 mutant with lower affinity for heparin exhibited a similar reduction of infectivity on several CHO cell lines, suggesting that the mutant uses an HSPG-mediated infection pathway (Maheshri *et al*., 2006). In addition, whereas the recovery of infectious virions from the column is similar for AAV2 and AAV8, dramatic differences occurred in the fraction of the genome-containing particles present in the flowthrough for these two serotypes. The large fraction of AAV2 genome-containing particles in the flowthrough could represent virions with an altered structural display of the His_6 tag that interferes with HSPG binding and hence viral infectivity, whereas AAV8 does not show a similar trend, suggesting this loop could be relatively less important for facilitating binding to cellular receptors. In addition, the contrasting results for these two AAV serotypes highlight the challenges that may occur when translating a peptide insertion from one AAV serotype to the analogous region in an alternative AAV serotype.

Three weeks after purified vector injection into the rat striatum, viral tropism and gene expression were similar for vectors packaged with His_6 AAV2 and wild-type capsid (Fig. 4A and B). Previous studies in the brain showed increased rAAV spread and volume accessed for AAV serotypes that do not bind HSPG (Davidson *et al*., 2000; Burger *et al*., 2004) or when low molecular weight heparin was coinfused with AAV2 (Nguyen *et al*., 2001; Hadaczek *et al*., 2004). Interestingly, in this study the reduced affinity of a fraction of His_6 AAV2 for heparin (Fig. 3A) did not translate into enhanced spread within the brain, which contains high amounts of HSPG, potentially because an even moderate affinity for heparan sulfate could be sufficient to hinder free diffusion of the vector. However, our data collectively demonstrate that the gene delivery properties of His_6 AAV2 and wild-type AAV capsid are comparable both *in vivo* and *in vitro*.

Robust production methods of highly purified rAAV vectors will enhance the applicability of AAV as a gene delivery vector while minimizing a host immune response. Prior work involving injection of rAAV vectors purified by CsCl, affinity, and ion-exchange methods has shown that AAV itself does not result in significant activation of macrophages, microglia, and CD4-positive or CD8-positive T lymphocytes (Peden *et al*., 2004; Sanftner *et al*., 2004). Purification of His_6 AAV2 via IMAC resulted in similar basal levels of immune cell activation, further supporting the use of His_6 AAV2 vectors for *in vivo* gene delivery (Fig. 4E and F).

In summary, we report the construction of novel His_6 AAV mutants for two serotypes that can be easily and effectively purified directly from cell lysate, using a single-step IMAC column for safe and efficient *in vitro* and *in vivo* gene delivery. His_6 tags may prove useful for other applications, such as the attachment of fluorophore via a Ni-NTA linkage (Kapanidis *et al*., 2001) for viral tracking, or for the localization of viral vectors to cells expressing pseudo-His tag receptors (Grandi *et al*., 2004). In addition, the random peptide insertion approach described in this work has significant promise for viral vector engineering, but its application to AAV may require optimization of peptide size and flanking sequences before use. With such adaptations, it may allow for the identification of novel insertion sites within other AAV serotypes. Ultimately, the combination of rational design and large diverse viral libraries will aid in the engineering of viral vectors for improved gene delivery.

ACKNOWLEDGMENTS

The authors thank Eric Steen for technical assistance. This work was supported by UC Discovery BIO04-10472, an NSF Graduate Fellowship (to J.T.K.), and NIH EB003007.

REFERENCES

ARNOLD, G.S., SASSER, A.K., STACHLER, M.D., and BARTLETT, J.S. (2006). Metabolic biotinylation provides a unique platform for the purification and targeting of multiple AAV vector serotypes. Mol. Ther. **14,** 97–106.

AURICCHIO, A., HILDINGER, M., O'CONNOR, E., GAO, G.P., and WILSON, J.M. (2001). Isolation of highly infectious and pure adeno-associated virus type 2 vectors with a single-step gravity-flow column. Hum. Gene Ther. **12,** 71–76.

BRUMENT, N., MORENWEISER, R., BLOUIN, V., TOUBLANC, E., RAIMBAUD, I., CHEREL, Y., FOLLIOT, S., GADEN, F., BOULANGER, P., KRONER-LUX, G., MOULLIER, P., ROLLING, F., and SALVETTI, A. (2002). A versatile and scalable two-step ion-exchange chromatography process for the purification of recombinant adeno-associated virus serotypes-2 and -5. Mol. Ther. **6,** 678–686.

BRUNE, W., MENARD, C., HOBOM, U., ODENBREIT, S., MESSERLE, M., and KOSZINOWSKI, U.H. (1999). Rapid identification of essential and nonessential herpesvirus genes by direct transposon mutagenesis. Nat. Biotechnol. **17,** 360–364.

BURGER, C., GORBATYUK, O.S., VELARDO, M.J., PEDEN, C.S., WILLIAMS, P., ZOLOTUKHIN, S., REIER, P.J., MANDEL, R.J., and MUZYCZKA, N. (2004). Recombinant AAV viral vectors pseudotyped with viral capsids from serotypes 1, 2, and 5 display differential efficiency and cell tropism after delivery to different regions of the central nervous system. Mol. Ther. **10,** 302–317.

CHIORINI, J.A., KIM, F., YANG, L., and KOTIN, R.M. (1999). Cloning and characterization of adeno-associated virus type 5. J. Virol. **73,** 1309–1319.

CLARK, K.R., LIU, X., McGRATH, J.P., and JOHNSON, P.R. (1999). Highly purified recombinant adeno-associated virus vectors are biologically active and free of detectable helper and wild-type viruses. Hum. Gene Ther. **10,** 1031–1039.

CONLON, T.J., COSSETTE, T., ERGER, K., CHOI, Y.K., CLARKE, T., SCOTT-JORGENSEN, M., SONG, S., CAMPBELL-THOMPSON, M., CRAWFORD, J., and FLOTTE, T.R. (2005). Efficient hepatic delivery and expression from a recombinant adeno-associated virus 8 pseudotyped α_1-antitrypsin vector. Mol. Ther. **12,** 867–875.

DAVIDSON, B.L., STEIN, C.S., HETH, J.A., MARTINS, I., KOTIN, R.M., DERKSEN, T.A., ZABNER, J., GHODSI, A., and CHIORINI, J.A. (2000). Recombinant adeno-associated virus type 2, 4, and 5 vectors: Transduction of variant cell types and regions in the mammalian central nervous system. Proc. Natl. Acad. Sci. U.S.A. **97,** 3428–3432.

ESKO, J.D., STEWART, T.E., and TAYLOR, W.H. (1985). Animal cell mutants defective in glycosaminoglycan biosynthesis. Proc. Natl. Acad. Sci. U.S.A. **82,** 3197–3201.

FIELDS, B.N., KNIPE, D.M., HOWLEY, P.M., and GRIFFIN, D.E. (2001). *Fields Virology*. (Lippincott Williams & Wilkins, Philadelphia).

FLOTTE, T.R., AFIONE, S.A., CONRAD, C., McGRATH, S.A., SOLOW, R., OKA, H., ZEITLIN, P.L., GUGGINO, W.B., and CARTER, B.J. (1993). Stable *in vivo* expression of the cystic fibrosis transmembrane conductance regulator with an adeno-associated virus vector. Proc. Natl. Acad. Sci. U.S.A. **90,** 10613–10617.

GAO, G., VANDENBERGHE, L.H., ALVIRA, M.R., LU, Y., CALCEDO, R., ZHOU, X., and WILSON, J.M. (2004). Clades of adeno-

associated viruses are widely disseminated in human tissues. J. Virol. **78,** 6381–6388.

GIROD, A., RIED, M., WOBUS, C., LAHM, H., LEIKE, K., KLEINSCHMIDT, J., DELEAGE, G., and HALLEK, M. (1999). Genetic capsid modifications allow efficient re-targeting of adeno-associated virus type 2. Nat. Med. **5,** 1052–1056.

GRANDI, P., WANG, S., SCHUBACK, D., KRASNYKH, V., SPEAR, M., CURIEL, D.T., MANSERVIGI, R., and BREAKEFIELD, X.O. (2004). HSV-1 virions engineered for specific binding to cell surface receptors. Mol. Ther. **9,** 419–427.

GRIFMAN, M., TREPEL, M., SPEECE, P., GILBERT, L.B., ARAP, W., PASQUALINI, R., and WEITZMAN, M.D. (2001). Incorporation of tumor-targeting peptides into recombinant adeno-associated virus capsids. Mol. Ther. **3,** 964–975.

GRIMM, D., KERN, A., RITTNER, K., and KLEINSCHMIDT, J.A. (1998). Novel tools for production and purification of recombinant adenoassociated virus vectors. Hum. Gene Ther. **9,** 2745–2760.

HADACZEK, P., MIREK, H., BRINGAS, J., CUNNINGHAM, J., and BANKIEWICZ, K. (2004). Basic fibroblast growth factor enhances transduction, distribution, and axonal transport of adeno-associated virus type 2 vector in rat brain. Hum. Gene Ther. **15,** 469–479.

HU, Y.C., TSAI, C.T., CHUNG, Y.C., LU, J.T., and HSU, J.T.A. (2003). Generation of chimeric baculovirus with histidine-tags displayed on the envelope and its purification using immobilized metal affinity chromatography. Enzyme Microb. Technol. **33,** 445–452.

HUTTNER, N.A., GIROD, A., PERABO, L., EDBAUER, D., KLEINSCHMIDT, J.A., BUNING, H., and HALLEK, M. (2003). Genetic modifications of the adeno-associated virus type 2 capsid reduce the affinity and the neutralizing effects of human serum antibodies. Gene Ther. **10,** 2139–2147.

KALUDOV, N., HANDELMAN, B., and CHIORINI, J.A. (2002). Scalable purification of adeno-associated virus type 2, 4, or 5 using ion-exchange chromatography. Hum. Gene Ther. **13,** 1235–1243.

KAPANIDIS, A.N., EBRIGHT, Y.W., and EBRIGHT, R.H. (2001). Site-specific incorporation of fluorescent probes into protein: Hexahistidine-tag-mediated fluorescent labeling with $(Ni^{2+}$:nitrilotriacetic acid$)_n$–fluorochrome conjugates. J. Am. Chem. Soc. **123,** 12123–12125.

KAPLITT, M.G., LEONE, P., SAMULSKI, R.J., XIAO, X., PFAFF, D.W., O'MALLEY, K.L., and DURING, M.J. (1994). Long-term gene expression and phenotypic correction using adeno-associated virus vectors in the mammalian brain. Nat. Genet. **8,** 148–154.

KASPAR, B.K., LLADO, J., SHERKAT, N., ROTHSTEIN, J.D., and GAGE, F.H. (2003). Retrograde viral delivery of IGF-1 prolongs survival in a mouse ALS model. Science **301,** 839–842.

KAY, M.A., MANNO, C.S., RAGNI, M.V., LARSON, P.J., COUTO, L.B., McCLELLAND, A., GLADER, B., CHEW, A.J., TAI, S.J., HERZOG, R.W., ARRUDA, V., JOHNSON, F., SCALLAN, C., SKARSGARD, E., FLAKE, A.W., and HIGH, K.A. (2000). Evidence for gene transfer and expression of factor IX in haemophilia B patients treated with an AAV vector. Nat. Genet. **24,** 257–261.

KERN, A., SCHMIDT, K., LEDER, C., MULLER, O.J., WOBUS, C.E., BETTINGER, K., VON DER LIETH, C.W., KING, J.A., and KLEINSCHMIDT, J.A. (2003). Identification of a heparin-binding motif on adeno-associated virus type 2 capsids. J. Virol. **77,** 11072–11081.

KLEIN, R.L., DAYTON, R.D., LEIDENHEIMER, N.J., JANSEN, K., GOLDE, T.E., and ZWEIG, R.M. (2006). Efficient neuronal gene transfer with AAV8 leads to neurotoxic levels of tau or green fluorescent proteins. Mol. Ther. **13,** 517–527.

LACY, H.M., and SANDERSON, R.D. (2002). 6×His promotes binding of a recombinant protein to heparan sulfate. Biotechniques **32,** 254, 256, 258.

LEE, K.K., FITCH, C.A., LECOMTE, J.T., and GARCIA-MORENO, E.B. (2002). Electrostatic effects in highly charged proteins: Salt sensitivity of pK_a values of histidines in staphylococcal nuclease. Biochemistry **41,** 5656–5667.

MAHESHRI, N., KOERBER, J.T., KASPAR, B.K., and SCHAFFER, D.V. (2006). Directed evolution of adeno-associated virus yields enhanced gene delivery vectors. Nat. Biotechnol. **24,** 198–204.

MANNO, C.S., CHEW, A.J., HUTCHISON, S., LARSON, P.J., HERZOG, R.W., ARRUDA, V.R., TAI, S.J., RAGNI, M.V., THOMPSON, A., OZELO, M., COUTO, L.B., LEONARD, D.G., JOHNSON, F.A., McCLELLAND, A., SCALLAN, C., SKARSGARD, E., FLAKE, A.W., KAY, M.A., HIGH, K.A., and GLADER, B. (2003). AAV-mediated factor IX gene transfer to skeletal muscle in patients with severe hemophilia B. Blood **101,** 2963–2972.

MANNO, C.S., ARRUDA, V.R., PIERCE, G.F., GLADER, B., RAGNI, M., RASKO, J., OZELO, M.C., HOOTS, K., BLATT, P., KONKLE, B., DAKE, M., KAYE, R., RAZAVI, M., ZAJKO, A., ZEHNDER, J., NAKAI, H., CHEW, A., LEONARD, D., WRIGHT, J.F., LESSARD, R.R., SOMMER, J.M., TIGGES, M., SABATINO, D., LUK, A., JIANG, H., MINGOZZI, F., COUTO, L., ERTL, H.C., HIGH, K.A., and KAY, M.A. (2006). Successful transduction of liver in hemophilia by AAV-Factor IX and limitations imposed by the host immune response. Nat. Med. **12,** 342–347.

MULLER, O.J., KAUL, F., WEITZMAN, M.D., PASQUALINI, R., ARAP, W., KLEINSCHMIDT, J.A., and TREPEL, M. (2003). Random peptide libraries displayed on adeno-associated virus to select for targeted gene therapy vectors. Nat. Biotechnol. **21,** 1040–1046.

NGUYEN, J.B., SANCHEZ-PERNAUTE, R., CUNNINGHAM, J., and BANKIEWICZ, K.S. (2001). Convection-enhanced delivery of AAV-2 combined with heparin increases TK gene transfer in the rat brain. Neuroreport **12,** 1961–1964.

OPIE, S.R., WARRINGTON, K.H., JR., AGBANDJE-McKENNA, M., ZOLOTUKHIN, S., and MUZYCZKA, N. (2003). Identification of amino acid residues in the capsid proteins of adeno-associated virus type 2 that contribute to heparan sulfate proteoglycan binding. J. Virol. **77,** 6995–7006.

PARROTT, M.B., ADAMS, K.E., MERCIER, G.T., MOK, H., CAMPOS, S.K., and BARRY, M.A. (2003). Metabolically biotinylated adenovirus for cell targeting, ligand screening, and vector purification. Mol. Ther. **8,** 688–700.

PEDEN, C.S., BURGER, C., MUZYCZKA, N., and MANDEL, R.J. (2004). Circulating anti-wild-type adeno-associated virus type 2 (AAV2) antibodies inhibit recombinant AAV2 (rAAV2)-mediated, but not rAAV5-mediated, gene transfer in the brain. J. Virol. **78,** 6344–6359.

PERABO, L., BUNING, H., KOFLER, D.M., RIED, M.U., GIROD, A., WENDTNER, C.M., ENSSLE, J., and HALLEK, M. (2003). *In vitro* selection of viral vectors with modified tropism: The adeno-associated virus display. Mol. Ther. **8,** 151–157.

PORATH, J., CARLSSON, J., OLSSON, I., and BELFRAGE, G. (1975). Metal chelate affinity chromatography, a new approach to protein fractionation. Nature **258,** 598–599.

RABINOWITZ, J.E., XIAO, W., and SAMULSKI, R.J. (1999). Insertional mutagenesis of AAV2 capsid and the production of recombinant virus. Virology **265,** 274–285.

SAMULSKI, R.J., CHANG, L.S., and SHENK, T. (1989). Helper-free stocks of recombinant adeno-associated viruses: Normal integration does not require viral gene expression. J. Virol. **63,** 3822–3828.

SANFTNER, L.M., SUZUKI, B.M., DOROUDCHI, M.M., FENG, L., McCLELLAND, A., FORSAYETH, J.R., and CUNNINGHAM, J. (2004). Striatal delivery of rAAV-hAADC to rats with preexisting immunity to AAV. Mol. Ther. **9,** 403–409.

SARKAR, R., MUCCI, M., ADDYA, S., TETREAULT, R., BELLINGER, D.A., NICHOLS, T.C., and KAZAZIAN, H.H., Jr. (2006). Long-term efficacy of adeno-associated virus serotypes 8 and 9 in hemophilia a dogs and mice. Hum. Gene Ther. **17,** 427–439.

SHI, W., ARNOLD, G.S., and BARTLETT, J.S. (2001). Insertional mutagenesis of the adeno-associated virus type 2 (AAV2) capsid gene and generation of AAV2 vectors targeted to alternative cell-surface receptors. Hum. Gene Ther. **12,** 1697–1711.

SNYDER, R.O., XIAO, X., SAMULSKI, R.J. (1996). Production of recombinant adeno-associated viral vectors. *In* N. Dracopoli, Haines, J., Krof B., Moir, D., Morton C., Seidman, C., Seidman, J., and Smith, D., eds. *Current Protocols in Human Genetics* (John Wiley & Sons, New York) pp. 12.1.1–12.1.24.

SRIVASTAVA, A., LUSBY, E.W., and BERNS, K.I. (1983). Nucleotide sequence and organization of the adeno-associated virus 2 genome. J. Virol. **45,** 555–564.

WALTERS, R.W., YI, S.M., KESHAVJEE, S., BROWN, K.E., WELSH, M.J., CHIORINI, J.A., and ZABNER, J. (2001). Binding of adeno-associated virus type 5 to 2,3-linked sialic acid is required for gene transfer. J. Biol. Chem. **276,** 20610–20616.

WANG, Z., ZHU, T., QIAO, C., ZHOU, L., WANG, B., ZHANG, J., CHEN, C., LI, J., and XIAO, X. (2005). Adeno-associated virus serotype 8 efficiently delivers genes to muscle and heart. Nat. Biotechnol. **23,** 321–328.

WU, P., XIAO, W., CONLON, T., HUGHES, J., AGBANDJE-McKENNA, M., FERKOL, T., FLOTTE, T., and MUZYCZKA, N. (2000). Mutational analysis of the adeno-associated virus type 2 (AAV2) capsid gene and construction of AAV2 vectors with altered tropism. J. Virol. **74,** 8635–8647.

XIAO, X., LI, J., and SAMULSKI, R.J. (1998). Production of high-titer recombinant adeno-associated virus vectors in the absence of helper adenovirus. J. Virol. **72,** 2224–2232.

XIE, Q., BU, W., BHATIA, S., HARE, J., SOMASUNDARAM, T., AZZI, A., and CHAPMAN, M.S. (2002). The atomic structure of adeno-associated virus (AAV-2), a vector for human gene therapy. Proc. Natl. Acad. Sci. U.S.A. **99,** 10405–10410.

YE, K., JIN, S., ATAAI, M.M., SCHULTZ, J.S., and IBEH, J. (2004). Tagging retrovirus vectors with a metal binding peptide and one-step purification by immobilized metal affinity chromatography. J. Virol. **78,** 9820–9827.

YU, J.H., and SCHAFFER, D.V. (2006). Selection of novel vesicular stomatitis virus glycoprotein variants from a peptide insertion library for enhanced purification of retroviral and lentiviral vectors. J. Virol. **80,** 3285–3292.

ZHANG, H.G., XIE, J., DMITRIEV, I., KASHENTSEVA, E., CURIEL, D.T., HSU, H.C., and MOUNTZ, J.D. (2002). Addition of six-His-tagged peptide to the C terminus of adeno-associated virus VP3 does not affect viral tropism or production. J. Virol. **76,** 12023–12031.

ZOLOTUKHIN, S., BYRNE, B.J., MASON, E., ZOLOTUKHIN, I., POTTER, M., CHESNUT, K., SUMMERFORD, C., SAMULSKI, R.J., and MUZYCZKA, N. (1999). Recombinant adeno-associated virus purification using novel methods improves infectious titer and yield. Gene Ther. **6,** 973–985.

Address reprint requests to:
Dr. David V. Schaffer
Department of Chemical Engineering and
Helen Wills Neuroscience Institute
University of California, Berkeley
Berkeley, CA 94720

E-mail: schaffer@berkeley.edu

Received for publication September 30, 2006; accepted after revision December 4, 2006.

Published online: April 13, 2007.